

Thiocyanate-Bridged Transition-Metal Polymers. 1. Structure and Low-Temperature Magnetic Behavior of (Bipyridyl)iron(II) Thiocyanate: Fe(bpy)(NCS)₂

BRUCE W. DOCKUM and WILLIAM MICHAEL REIFF*

Received April 17, 1981

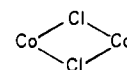
Fe(bpy)(NCS)₂ (bpy = 2,2'-bipyridine) has been prepared by the thermolytic decomposition of the monomeric bis(bipyridyl) complex Fe(bpy)₂(NCS)₂. Studies using Mössbauer, near-infrared-visible, and infrared spectroscopies indicate that the compound is a polymer with zigzag chains containing stepwise metal-thiocyanate bridging groups and six-coordinate metal centers. Variable-temperature susceptibility measurements (1.4–303 K) for Fe(bpy)(NCS)₂ show the presence of a broad susceptibility maximum at ~18 K. This maximum plus the rapid decrease in the moment indicates antiferromagnetic exchange in the polymer chains. Such exchange is proposed to be pairwise in nature, and with use of the Heisenberg-Dirac-Van Vleck dipolar coupling model, the exchange energy, *J*, is estimated to be -2.7 cm⁻¹. Zero-field Mössbauer spectra show that Fe(bpy)(NCS)₂ exhibits no evidence of three-dimensional order for temperatures as low as 1.6 K. High-field spectra indicate a negative quadrupole interaction and rapid relaxation at both 77 and 4.2 K. The Mössbauer spectra also indicate a structure transformation between two distinct forms of the compound in the range 200–130 K.

Introduction

Recently, there has been interest in the magnetic properties of compounds containing bridging pseudohalide anions such as the thiocyanate ion (NCS⁻). In studies now available, it has been shown that the thiocyanate bridge can provide a pathway for magnetic exchange between metal atoms in dimeric and polymeric transition-metal compounds. For example, positive (ferromagnetic) magnetic exchange occurs between metal atoms in the thiocyanate-bridged nickel dimers [Ni(en)₂(NCS)]₂I₂¹ and [Ni(tren)(NCS)]₂(BPh₄)₂² (en = ethylenediamine; tren = 2,2',2''-triaminotriethylamine). Also, Fe(py)₂(NCS)₂ (py = pyridine), a linear chain polymer,³ exhibits strong ferromagnetic interactions along the iron-thiocyanate chains with relatively weak antiferromagnetic exchange between chains, three-dimensionally ordering at *T*_N ~ 6.0 K.⁴ Recently, a detailed single-crystal structure, heat capacity, proton magnetic resonance, and magnetic susceptibility study indicates that Mn(C₂H₅OH)₂(NCS)₂ behaves as a two-dimensional Heisenberg magnet with negative intralayer exchange (*J*/*k* = -0.88 K) and orders at ~10.3 K.⁵ In each of the preceding examples, all of the thiocyanate anions are bridging. However, there are polymers in which only a fraction of the available thiocyanate anions is bridging. This results in a more dilute magnetic system with weaker magnetic interactions between metal ions. Specific examples of the latter are Cu(en)(NCS)₂⁶ and Cu(bpy)(NCS)₂.⁶

Fe(bpy)(NCS)₂ (bpy = 2,2'-bipyridine) is a member of a new series of metal bipyridyl thiocyanate compounds that have been prepared in our laboratory to study the magnetic properties of a system of zigzag polymers that results from the cis nitrogen coordination of ligands such as 2,2'-bipyridine.⁷ Extensive studies using spectroscopic, magnetic, and X-ray crystallographic methods have been done for a closely related series of compounds, the mono(diimine) metal halides, MLX₂, where M is divalent Mn, Fe, Co, or Ni; L is a diimine ligand, either 1,10-phenanthroline (phen) or 2,2'-bipyridine; and X

is Cl, Br, or I.⁸⁻¹³ The structures for these halides are expected to be very similar to that recently determined for Co(bpy)Cl₂,¹² which is shown in Figure 1. Co(bpy)Cl₂ is an infinite polymer containing zigzag chains of cobalt atoms linked together by pairs of Cl atoms. These



bridging groups are near orthogonal. The dihedral angle between such bridge units is ~89°, and the angle subtended by three successive metal atoms of the polymer chain is ~130°. The remaining two positions around the cobalt atom are occupied by two nitrogen atoms from 2,2'-bipyridine, forming a distorted *cis*-CoN₂Cl₂ center. Ferromagnetic exchange interactions are evident in the magnetic behavior of the mono(diimine) metal halides; for example, Fe(phen)Cl₂,^{8,9} Fe(bpy)Cl₂,^{9,10} and Co(bpy)Cl₂¹² order three-dimensionally as ferromagnets. By analogy to the foregoing halide compounds, Fe(bpy)(NCS)₂ is expected to be polymeric with a structure generally resembling that for Co(bpy)Cl₂; i.e., no gross changes occur in the stepwise zigzag polymeric chain and its packing. However, substitution of the larger, more complex thiocyanate anion for the halide ion is expected to increase the metal-metal distance in bridge units from 3.7 to ~6.0 Å and may result in changes in the magnitude and/or sign of the magnetic exchange. We now present data bearing on the structure and the magnetic properties of Fe(bpy)(NCS)₂.

Experimental Section

Preparation of Fe(bpy)(NCS)₂. Fe(bpy)(NCS)₂ was prepared by thermolysis of the dark maroon Fe(bpy)₂(NCS)₂¹³ at ~200 °C under vacuum for 4 days. The heating was stopped when the product no longer changed color and weight. The brown-orange product was analyzed as Fe(bpy)(NCS)₂. Anal. Calcd for Fe(bpy)(NCS)₂: C, 43.92; H, 2.46; N, 17.07. Found: C, 43.68; H, 2.45; N, 16.93. The

- (1) A. P. Ginsberg, R. L. Martin, R. W. Brookes, and R. C. Sherwood, *Inorg. Chem.*, **11**, 2884 (1972).
- (2) D. M. Duggan and D. N. Hendrickson, *Inorg. Chem.*, **13**, 2929 (1974).
- (3) W. M. Reiff, R. B. Frankel, B. F. Little, and G. J. Long, *Inorg. Chem.*, **13**, 2153 (1974).
- (4) S. Foner, R. B. Frankel, E. J. McNiff, Jr., W. M. Reiff, B. F. Little, and G. J. Long, *AIP Conf. Proc.*, No. **24**, 363 (1975).
- (5) J. N. McElearney, L. L. Balagot, J. A. Muir, and R. D. Spence, *Phys. Rev. B*, **19**, 306 (1979).
- (6) W. M. Reiff, H. Wong, B. Dockum, T. Brennan, and C. Cheng, *Inorg. Chim. Acta*, **30**, 69 (1978).
- (7) B. W. Dockum, Ph.D. Dissertation, Department of Chemistry, Northeastern University, Boston, MA, 1977.

- (8) W. M. Reiff and S. Foner, *J. Am. Chem. Soc.*, **95**, 260 (1973).
- (9) W. M. Reiff, B. Dockum, C. Torardi, S. Foner, R. B. Frankel, and M. A. Weber, *ACS Symp. Ser.*, No. **5**, 205 (1974).
- (10) W. M. Reiff, B. Dockum, M. A. Weber, and R. B. Frankel, *Inorg. Chem.*, **14**, 800 (1975).
- (11) W. M. Reiff, H. Wong, and C. Cheng, paper presented at the 173rd National Meeting of the American Chemical Society New Orleans, LA, March 1977.
- (12) W. M. Reiff, H. Wong, G. Eisman, W. Rode, and B. Foxman, manuscript in preparation, and Abstracts, 179th National Meeting of the American Chemical Society Houston, TX, March 1980, No. INOR 22.
- (13) E. König, K. Madeja, and K. J. Watson, *J. Am. Chem. Soc.*, **90**, 1146 (1968).

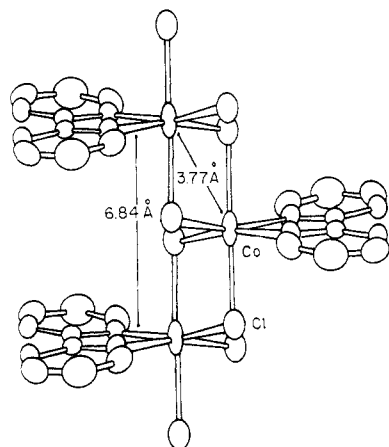


Figure 1. Schematic of the structure of $\text{Co}(\text{bpy})\text{Cl}_2$.

Table I. Optical Spectra of Some Iron(II) Imine and Diimine Compounds

compd ^{a,b}	band maxima and relative intensities ^d	ref
$\text{Fe}(\text{bpy})(\text{NCS})_2$ (A)	5250, ~10750 (w, sh)	e
(B)	~5000, ~10500 (w, sh)	
$\text{Fe}(\text{py})_2(\text{NCS})_2$	7200, 13100, 21700 (s, br)	3
$\text{Fe}(\text{biq})(\text{NCS})_2$	6000 (sh), 6900 (vs), 17600 (sh), 18700 (sh)	7
$\text{Fe}(2,9\text{-dmp})(\text{NCS})_2$	5600 (w, sh), 6940 (vs), 19200 (s, sh)	7
$\text{Fe}(\text{biq})\text{Cl}_2$	6000 (s, sh), 7100 (vs)	7

^a bpy = 2,2'-bipyridine, py = pyridine, biq = 2,2'-biquinoline, 2,9-dmp = 2,9-dimethyl-1,10-phenanthroline. ^b A = spectrum taken with a concentrated mull, B = spectrum taken with a dilute mull. ^c Positions in cm^{-1} . ^d w = weak, vs = very strong, m = medium, sh = shoulder, s = strong, br = broad. ^e This work.

analyses were done by Galbraith Labs., Knoxville, TN.

Physical Measurements. Magnetic susceptibility measurements were made from 1.4 to 300 K by the Faraday method. A description of the Faraday apparatus has been reported elsewhere.¹⁴ The apparatus was calibrated with $\text{HgCo}(\text{NCS})_4$.¹⁵⁻¹⁷ Diamagnetic corrections to the susceptibility of $\text{Fe}(\text{bpy})(\text{NCS})_2$ were calculated from Pascal's constants;¹⁸ for $\text{Fe}(\text{bpy})(\text{NCS})_2$, $\chi_{\text{dia}} = -180 \times 10^{-6}$ cgs mol^{-1} .

The Mössbauer spectrometer used in this work has also been described previously.^{14,19} The Mössbauer spectrometer used in this investigation was calibrated by using 99.99% (6 μm thick) iron foil. The isomer shift values are quoted relative to the center of the hyperfine pattern of the iron foil at room temperature. The spectra were fit to Lorentzian lines by using a modified version of the program of Stone.^{20,21}

Optical spectra were determined with a Cary 14 recording spectrometer. Samples were prepared as mulls by using Halocarbon 25-SS grease (Halocarbon Products Corp., Hackensack, NJ) with finely ground sample that was suspended between two UV-grade quartz plates.

Infrared spectra between 4000 and 200 cm^{-1} were obtained on a Perkin-Elmer Model 567 spectrometer. Samples were taken as mineral oil mulls on a single NaCl plate, a single polyethylene disk, or as KBr pellets.

X-ray powder patterns were determined with a General Electric Model XRD-6 diffractometer.

Results and Discussion

Optical Spectra. The optical spectra of $\text{Fe}(\text{bpy})(\text{NCS})_2$ were taken at room temperature with mulls having different

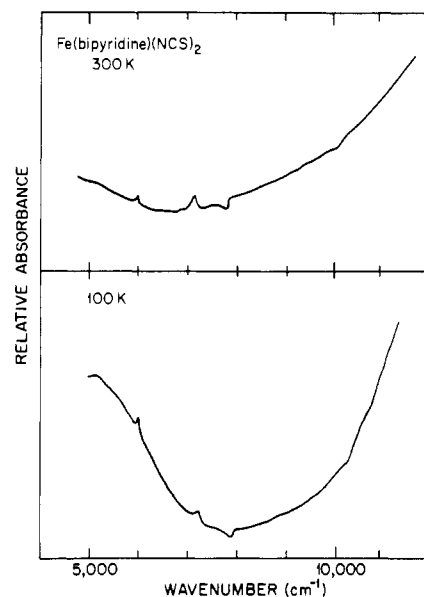
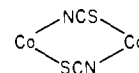


Figure 2. Top: Room-temperature optical spectrum of $\text{Fe}(\text{bpy})_2(\text{NCS})_2$ taken with a concentrated mull. Bottom: 100 K optical spectrum of $\text{Fe}(\text{bpy})_2(\text{NCS})_2$ taken with a dilute mull.

concentrations. The band maxima are presented in Table I. The spectra show two bands, one well-resolved band at ~ 5000 cm^{-1} and a second band centered at ~ 11000 cm^{-1} , which is seen as part of the slope of an intense charge-transfer band; see Figure 2. The center of this charge-transfer band could not be measured. The pattern of this spectrum is similar to that found in the spectrum for $\text{Fe}(\text{py})_2(\text{NCS})_2$ except that the bands for $\text{Fe}(\text{py})_2(\text{NCS})_2$ are blue shifted by ~ 2000 cm^{-1} . The spectrum of $\text{Fe}(\text{py})_2(\text{NCS})_2$ shows two bands at 7200 and 13100 cm^{-1} (see Table I); the latter band is superimposed on a charge-transfer band centered at 21700 cm^{-1} .³ This charge-transfer band may be the result of small amounts of iron(III) thiocyanate impurity similar in character to the $\text{Fe}(\text{NCS})_6^{3-}$ anion, which is known to exhibit a charge-transfer band at 400 Å. Comparison of the X-ray powder patterns of $\text{Co}(\text{py})_2(\text{NCS})_2$ and $\text{Fe}(\text{py})_2(\text{NCS})_2$ shows that these two compounds are isomorphous. From a single-crystal study,²² the structure of $\text{Co}(\text{py})_2(\text{NCS})_2$ is articulated from



bridging units forming a *linear chain* with trans-axial pyridine group coordinated to the cobalt center. $\text{Fe}(\text{py})_2(\text{NCS})_2$ has a similar structure with a six-coordinate $\text{FeN}_2\text{N}'_2\text{S}_2$ chromophore. The gross features of the spectra of $\text{Fe}(\text{bpy})(\text{NCS})_2$ and $\text{Fe}(\text{py})_2(\text{NCS})_2$ are similar which indicates that $\text{Fe}(\text{bpy})(\text{NCS})_2$ also contains a *six-coordinate* $\text{FeN}_2\text{N}'_2\text{S}_2$ chromophore, but one of even lower symmetry as a result of the cis imine nitrogen from 2,2'-bipyridine and of having a lower ligand field strength than for $\text{Fe}(\text{py})_2(\text{NCS})_2$. Before concluding this section, the possibility of a four-coordinate iron center for $\text{Fe}(\text{bpy})(\text{NCS})_2$ should be considered. If the spectrum for $\text{Fe}(\text{bpy})(\text{NCS})_2$ is compared to that for some pseudotetrahedral iron(II) systems containing diimine ligands such as $\text{Fe}(2,9\text{-dmp})(\text{NCS})_2$,⁷ $\text{Fe}(2,9\text{-dmp})\text{Cl}_2$,¹⁰ $\text{Fe}(\text{biq})\text{Cl}_2$,⁷ and $\text{Fe}(\text{biq})(\text{NCS})_2$,⁷ (2,9-dmp = 2,9-dimethyl-1,10-phenanthroline and biq = 2,2'-biquinoline) (see Table I), they are found to be quite different. The spectra of these pseudotetrahedral compounds exhibit intense bands centered at ~ 7000 cm^{-1} , corresponding to a broadened and split $^5\text{E} \rightarrow$

- (14) W. M. Reiff and C. Cheng, *Inorg. Chem.*, **16**, 2097 (1977).
 (15) B. N. Figgis and R. S. Nyholm, *J. Chem. Soc.*, 419 (1958).
 (16) H. St. Rade, *J. Phys. Chem.*, **77**, 424 (1973).
 (17) D. B. Brown, V. H. Crawford, J. W. Hall, and W. E. Hatfield, *J. Phys. Chem.*, **81**, 1303 (1977).
 (18) B. N. Figgis and J. Lewis in "Modern Coordination Chemistry", J. Lewis and R. G. Wilkins, Eds., Wiley, New York, 1960, p 403.
 (19) C. Cheng, H. Wong, and W. M. Reiff, *Inorg. Chem.*, **16**, 819 (1977).
 (20) G. M. Bancroft, A. G. Maddock, W. K. Ong, R. H. Prince, and A. J. Stone, *J. Chem. Soc. A*, 1966 (1967).
 (21) D. Foster and D. M. L. Goodgame, *J. Chem. Soc.*, 268 (1965).

- (22) M. A. Porai-Koshits and G. N. Tishchenko, *Sov. Phys.—Crystallogr. (Engl. Transl.)*, **4**, 216 (1960).

Table II. Infrared Spectral Results for Fe(bpy)(NCS)₂ and Fe(bpy)₂(NCS)₂

band maxima, ^a cm ⁻¹		assignment
Fe(bpy)(NCS) ₂	Fe(bpy) ₂ (NCS) ₂	
2110 (s, sh)		N-C stretch, ν ₁ (NCS)
2080 (vs)	2062 (s)	
798 (w, br)	804 (w)	C-S stretch, ν ₃ (NCS)
480 (m)	478 (m)	N-C-S stretch, δ (NCS)
414 (m)		bipyridine band
284 (m, sh)		Fe-N(NCS) stretch Fe-N(bpy) stretch
265 (m)		
251 (m, sh)		

^a w = weak, m = medium, s = strong, vs = very strong, sh = shoulder, br = broad.

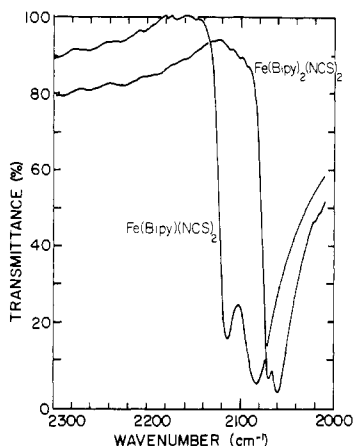


Figure 3. Infrared spectra of Fe(bpy)(NCS)₂ and Fe(bpy)₂(NCS)₂ at ~2000 cm⁻¹.

⁵T₂ transition in C_{2v} symmetry. This band does not change appreciably when NCS⁻ is substituted for Cl⁻. The strong band at ~7000 cm⁻¹ is not observed in the spectrum of Fe(bpy)(NCS)₂. A six-coordinate iron environment for Fe(bpy)(NCS)₂ is further supported by the Mössbauer data to be discussed.

Infrared Spectra. The principal infrared bands for Fe(bpy)(NCS)₂ and Fe(bpy)₂(NCS)₂ are presented in Table II. Figure 3 shows the spectral region around 2000 cm⁻¹ for Fe(bpy)(NCS)₂ and its precursor Fe(bpy)₂(NCS)₂. The region near 2000 cm⁻¹ is assigned to the C-N stretching mode, and the exact position of this band can be useful in determining the nature of the thiocyanate coordination. In Fe(bpy)₂(NCS)₂, this band is found at ~2062 cm⁻¹ and is characteristic of metal-nitrogen bonding for terminal thiocyanate.^{13,23} In contrast, there are two bands at 2110 and 2080 cm⁻¹ in the spectrum of Fe(bpy)(NCS)₂, characteristic of metal-nitrogen and metal-sulfur bonding as expected to be found in thiocyanate-bridged polymers.²³ Similar bands are found in (linear chain) Fe(py)₂(NCS)₂. Thus, in conjunction with the optical spectra, the infrared data also support a FeN₂N₂S₂ chromophore for Fe(bpy)(NCS)₂; i.e., Fe(bpy)(NCS)₂ is a polymer with thiocyanate bridging.

Zero-Field Mössbauer Spectra. Mössbauer spectra for Fe(bpy)(NCS)₂ have been measured for temperatures between 300 and 1.6 K. The parameters for these spectra are given in Table III. These measurements reveal that Fe(bpy)(NCS)₂ exists in two different structural forms: a high-temperature (HT) phase above ~212 K and a low-temperature (LT) phase below 130 K. The isomer shift values for both phases are near 1.0 mm/s, and each phase shows temperature-dependent quadrupole splitting that increases in magnitude as the tem-

perature decreases. Further comments about each separate phase are given below. Between ~212 and 130 K, the two phases coexist together in varying proportions (depending on the temperature) as demonstrated in Figure 4B,C. The complete details of the Mössbauer spectra in this temperature range and the structural phase transformation involved will be discussed in a future paper.

The spectrum for Fe(bpy)(NCS)₂ at 300 K, given in Figure 4A, exhibits a very small quadrupole splitting. The isomer shift is found at the lower end of the range of isomer shift values usually found for six-coordinate monomers^{24,25} and polymers^{3,10,26} containing high-spin (*S* = 2) iron(II), imine ligands, and halo or pseudohalo anions (0.93–1.1 mm/s). This low shift is probably the result of a somewhat increased 3d delocalization to covalently bonded sulfur. This results in a higher s-electron density at the iron nucleus and a lower isomer shift since the 3d-electron shielding of s electrons will be reduced. This is consistent with the optical and infrared spectral data, which point to a six-coordinate polymeric structure for Fe(bpy)(NCS)₂. It is interesting to note that there is a decrease in the isomer shift relative to the precursor Fe(bpy)₂(NCS)₂, an all nitrogen-bonded system containing cis-coordinated thiocyanate anions.²⁷ At 300 K the isomer shift of Fe(bpy)₂(NCS)₂ is 1.06¹³ while that of Fe(bpy)(NCS)₂ is 0.95 mm/s. A similar change occurs when Fe(py)₄(NCS)₂, a monomer containing trans *iso* thiocyanate anions and four pyridine (imine) nitrogen coordination,²⁸ is thermolytically converted to the linear chain polymer Fe(py)₂(NCS)₂ (δ = 1.05 to 1.00 mm/s)³. These changes reflect the increased covalency when two sulfur atoms replace two imine nitrogens from either 2,2'-bipyridine or two pyridine groups, respectively. The quadrupole splitting for Fe(bpy)(NCS)₂, Δ*E*_q = 0.394 mm/s, is small compared to Δ*E*_q = ~2.2 mm/s for the high-spin form of Fe(bpy)₂(NCS)₂.¹³ Such small quadrupole splittings have, however, been observed in other six-coordinate iron(II) compounds, i.e., the pseudooctahedral monomers Fe(isoquinoline)₄I₂ (Δ*E*_q = 0.40 mm/s)²⁴ and Fe(γ-picoline)₄I₂ (Δ*E*_q = 0.19 mm/s)²⁵ and the linear chain polymer Fe(py)₂Cl₂ (Δ*E*_q = 0.56 mm/s)²⁶. The small splitting observed for Fe(bpy)(NCS)₂ at 300 K clearly indicates that the iron electronic environment is essentially "cubic", with small axial and/or rhombic distortion of the ⁵T_{2g} ground state (in O_h symmetry) and with considerable thermal population of the low-lying, excited (orbital) states relative to the ground state. As the temperature decreases, these low-lying excited states become progressively depopulated, such that the HT phase of Fe(bpy)(NCS)₂ exhibits a highly temperature-dependent quadrupole splitting varying from 0.394 mm/s at ambient temperature to 1.127 mm/s at 140.08 K.

At 110.12 K, Fe(bpy)(NCS)₂ appears almost entirely in the low-temperature form; see Figure 4d. A larger quadrupole splitting is observed for this phase (see Table III) greater than 6 times that found for the HT phase at 300 K. This implies a more distorted six-coordinate iron environment for the LT phase. The isomer shift for the LT phase is also large (>1.0 mm/s). For many iron compounds, this increase in the isomer shift with decreasing temperature is due primarily to the second-order Doppler effect,²⁹ a relativistic effect involving the temperature. A Mössbauer spectrum with both the Fe(bpy)(NCS)₂ absorber and a γ-ray source cooled to 78 K was

(23) R. J. H. Clark and C. S. Williams, *Spectrochim. Acta*, **22**, 1081 (1966).

(24) R. M. Golding, K. F. Mok, and J. F. Duncan, *Inorg. Chem.*, **5**, 774 (1966).

(25) C. D. Burbridge, D. M. L. Goodgame, and M. Goodgame, *J. Chem. Soc. A*, 349 (1967).

(26) G. J. Long, D. L. Whitney, and J. E. Kennedy, *Inorg. Chem.*, **10**, 1406 (1971).

(27) E. König and K. J. Watson, *Chem. Phys. Lett.*, **6**, 457 (1970).

(28) I. Sotofte and S. E. Rasmussen, *Acta Chem. Scand.*, **21**, 2028 (1967).

(29) N. N. Greenwood and T. C. Gibb, "Mössbauer Spectroscopy", Chapman and Hall, London, 1971, p 50.

Table III. Mössbauer Parameters for the High- and Low-Temperature Phases of $\text{Fe}(\text{bpy})(\text{NCS})_2$

phase ^d	T, K	$\delta^{a,b}$	ΔE_q^c	$\Gamma_1^{a,c}$	$\Gamma_2^{a,c}$	Γ_1/Γ_2^c	A_1/A_2^c
LT	1.57	1.121	2.955	0.377	0.407	0.926	1.016
	4.2	1.124	2.934	0.324	0.326	0.994	1.016
	20.01	1.123	2.931	0.343	0.336	1.022	1.026
	41.51	1.120	2.925	0.307	0.305	1.006	1.037
	69.97	1.114	2.869	0.308	0.306	1.006	1.006
	110.12	1.104	2.579	0.358	0.345	1.038	1.048
	120.16	1.100	2.413	0.406	0.395	1.028	1.018
	130.28	1.094	2.179	0.492	0.501	0.982	1.002
HT	212.10	1.046	0.542	0.485	0.442	1.097	1.165
	300	0.949	0.394	0.299	0.296	1.010	1.057

^a These quantities are expressed in mm/s. ^b Relative to iron foil at 300 K. ^c Subscript 1 refers to the peak at lower velocities; subscript 2 refers to the peak at higher velocities. ^d HT phase 212.10 and 300 K; LT phase 1.57–130.28 K.

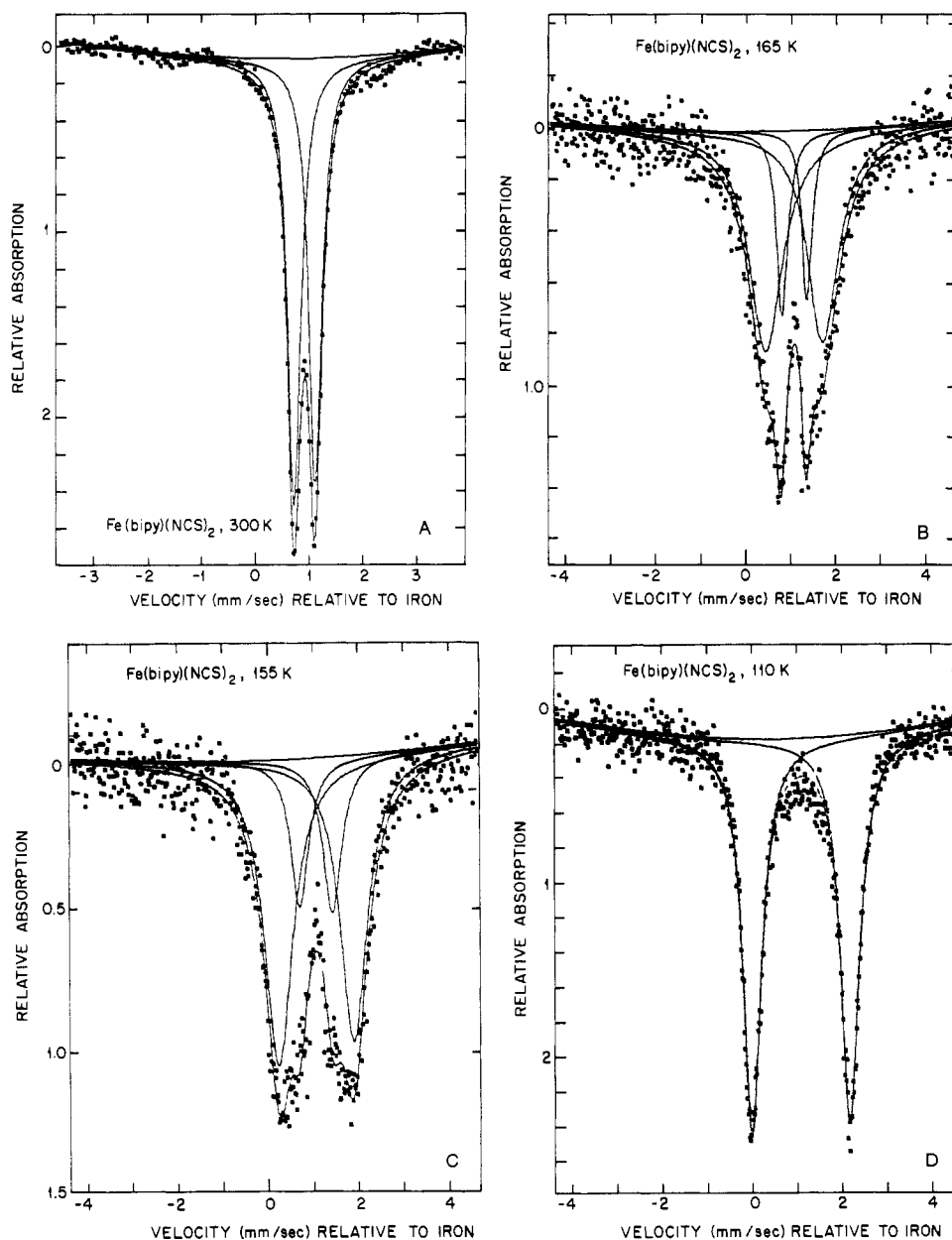


Figure 4. Zero-field Mössbauer spectra of $\text{Fe}(\text{bpy})(\text{NCS})_2$ at (A) 300 K, (B) 165 K, (C) 155 K, and (D) 110 K.

determined in order to eliminate the effects of the second-order Doppler effect on the isomer shift and to see if the structural phase transformation involves an increase in iron *coordination number*. The isomer shift for the latter spectrum (0.97 mm/s) is very close to the value for the HT phase at 300 K and clearly indicates no change of coordination number accompanies the foregoing phase transition.

High-Field Mössbauer Spectra. A Mössbauer spectrum of $\text{Fe}(\text{bpy})(\text{NCS})_2$ in an applied magnetic field of 60 kG was measured at 77 K and is shown in Figure 5. At this temperature $\text{Fe}(\text{bpy})(\text{NCS})_2$ is a rapidly relaxing paramagnet, and its spectrum shows the presence of two triplets representing a large asymmetry parameter, η . The most well-defined triplet appears to occur at higher velocities, implying a negative

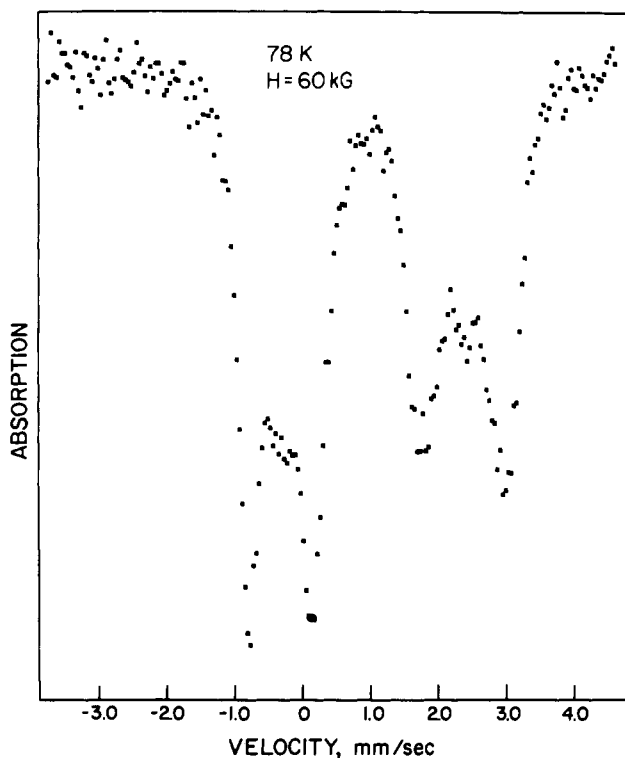


Figure 5. Mössbauer spectrum of $\text{Fe}(\text{bpy})(\text{NCS})_2$ at 78 K in an applied magnetic field of 60 kG.

quadrupole coupling constant (e^2Qq). Since the quadrupole moment for the $I = 3/2$ nuclear excited state is positive,³⁰ the principal component of the electric field gradient tensor, V_{zz} , is negative. The large quadrupole splitting and asymmetry parameter, η , support a highly distorted, nonaxial structure for the LT phase. In view of the distortion, asymmetry, and covalency of the iron coordination environment, it is difficult to relate the sign of V_{zz} to a simple, real, single-electron, ground-orbital wave function, i.e., d_{xy} , d_{xz} , etc. The orbital ground state is best viewed as a "mixed" orbital singlet of the form

$$\phi = \alpha|xy\rangle + \beta|xz\rangle + \gamma|yz\rangle$$

A complete description of the "ground state" would then involve a Boltzmann distribution of the "fourth" electron in the t_{2g} manifold over three such levels for both the HT and LT forms of $\text{Fe}(\text{bpy})(\text{NCS})_2$.

At 4.2 K, $\text{Fe}(\text{bpy})(\text{NCS})_2$ has a large quadrupole splitting in zero magnetic field; see Table III. In the presence of magnetic fields of 50 and 70 kG, the spectra are highly broadened, as seen in Figure 6. The very broad peak at higher velocities appears to be a triplet, again indicating V_{zz} is probably negative. The relatively small magnetic splittings of the spectral transitions at 4.2 K are the result of a nearly zero effective magnetic field, H_{eff} , at the iron nucleus in this compound. The effective field is made up of two contributions, the applied field, H_0 , and the internal field, H_n , or

$$H_{\text{eff}} = H_0 + H_n$$

In these spectra, the internal field apparently opposes the applied field, giving a near zero effective field and little apparent Zeeman splitting in the Mössbauer spectrum. The internal hyperfine field, which in itself is composed of a number of complicated controlling factors, can be estimated to have a lower limit in the range of 20–50 kG.

Structure of $\text{Fe}(\text{bpy})(\text{NCS})_2$. From the spectral data presented, $\text{Fe}(\text{bpy})(\text{NCS})_2$ is indicated to be a pseudocta-

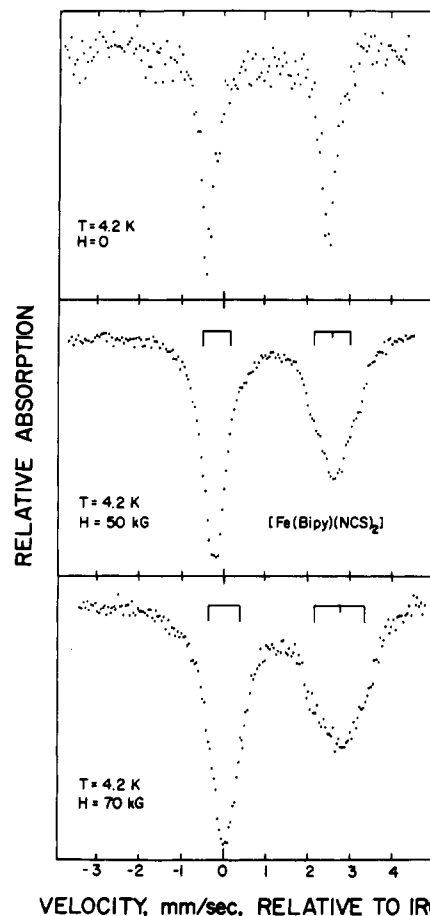
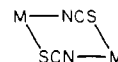


Figure 6. Mössbauer spectra of $\text{Fe}(\text{bpy})(\text{NCS})_2$ at 4.2 K in zero field and in fields of 50 and 70 kG.

hedral, thiocyanate-bridged polymer in which the local symmetry of the iron center is nonaxial. Unfortunately, a single-crystal X-ray study has not been possible to date. $\text{Fe}(\text{bpy})(\text{NCS})_2$, as synthesized herein, is a very fine polycrystalline powder, and attempts to grow single crystals by dissolving the powder in various solvents (dimethyl sulfoxide, nitrobenzene, nitromethane, and water, as examples) result in the decomposition of $\text{Fe}(\text{bpy})(\text{NCS})_2$ to the thermodynamically stable cation $\text{Fe}(\text{bpy})_3^{2+}$ plus other products. Furthermore, numerous attempts at direct solution preparation of $\text{Fe}(\text{bpy})(\text{NCS})_2$ using the appropriate 1:1 stoichiometry or an excess of metal have failed so far. It is the latter or slow gel diffusion of reactants that offer the greatest hope of obtaining a crystalline product for subsequent X-ray study. However, a probable structure for $\text{Fe}(\text{bpy})(\text{NCS})_2$ may be proposed by taking into account the available experimental data and the structures of known thiocyanate bridged polymers. Previous single-crystal studies of thiocyanate-bridged polymers have focused on the following: the magnetically 1-D systems $\text{Co}(\text{py})_2(\text{NCS})_2$,²² $\text{Cu}(\text{py})_2(\text{NCS})_2$,²² $\text{Co}(\text{NCS})_2 \cdot 3\text{H}_2\text{O}$,³¹ $\text{Ni}(\text{tim})_2(\text{NCS})_2$ (tim = 2-thioimidazolidinone),³² and $\text{Ni}(\text{tam})_2(\text{NCS})_2$ (tam = thioacetamide),³³ and the 2-D system $\text{Mn}(\text{C}_2\text{H}_5\text{OH})_2(\text{NCS})_2$.⁵ Each of the 1-D systems except for $\text{Ni}(\text{tam})_2(\text{NCS})_2$ is a linear chain polymer that contains the



bridging unit articulated in one direction with the nonbridging

(30) R. Ingalls, *Rev. Mod. Phys.*, **36**, 351 (1964).

(31) F. H. Cano, S. Garcia-Blanco, and A. Guerrero-Laverat, *Acta Crystallogr., Sect. B*, **B32**, 1526 (1976).

(32) M. Nardelli, G. F. Gasparri, A. Musatti, and A. Manfredotti, *Acta Crystallogr.*, **21**, 910 (1966).

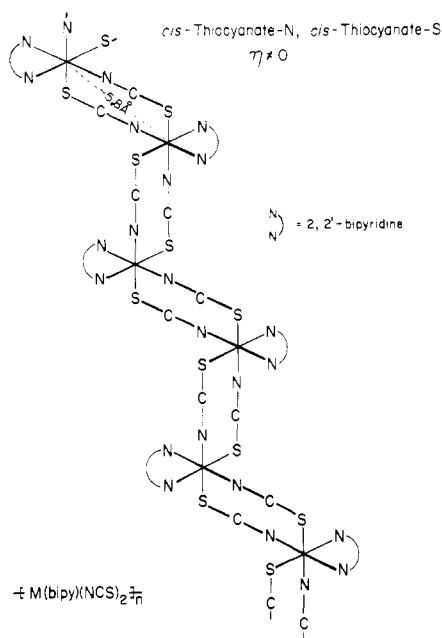


Figure 7. Zigzag chain structure for $\text{Fe}(\text{bpy})(\text{NCS})_2$.

ligand (pyridine, water, or 2-thioimidazolidinone) in a trans-axial position. For $\text{Mn}(\text{C}_2\text{H}_5\text{OH})_2(\text{NCS})_2$,⁵ the structure consists of sheets containing manganese atoms and bridging thiocyanate anions. The two ethanol ligands bond to the manganese in a trans-axial position above and below the sheets. The above structures (save one) cannot serve as complete analogues for the structure of $\text{Fe}(\text{bpy})(\text{NCS})_2$ since the imine nitrogen atoms from 2,2'-bipyridine must bond with the iron in cis coordination. The other system, $\text{Ni}(\text{tam})_2(\text{NCS})_2$, has a somewhat different structure³³ (space group $P3_121$) in that while its bridging groups are the same as for the linear chain systems, they are arranged in a near-orthogonal orientation to each other, forming a *helical* chain along the 3_1 screw axis. The sulfur atoms from the thioacetamide ligand bond with the nickel atom in a cis orientation forming $\text{NiN}_2\text{S}_2\text{S}'_2$ polyhedra with all sulfur atoms in a plane and the nitrogen atoms from the thiocyanate anions in a trans orientation. The structure of $\text{Ni}(\text{tam})_2(\text{NCS})_2$ can thus be a model for $\text{Fe}(\text{bpy})(\text{NCS})_2$ since the imine nitrogens from 2,2'-bipyridine are analogues of the cis thioacetamide S atoms in $\text{Ni}(\text{tam})_2(\text{NCS})_2$. Figure 7 presents another alternative structure for $\text{Fe}(\text{bpy})(\text{NCS})_2$ that we feel is perhaps more likely in view of the known structure of $\text{Co}(\text{bpy})\text{Cl}_2$. This structure contains a zigzag chain of near-orthogonal metal-thiocyanate bridging groups as found in $\text{Ni}(\text{tam})_2(\text{NCS})_2$, but they are joined together in a *stepwise zigzag* manner along the polymer chain. The symmetry of the iron coordination environment is C_1 and definitely nonaxial, in accord with the high-field Mössbauer spectrum at 78 K. It should be noted in passing that two other zigzag chain polymer structures are possible for $\text{Fe}(\text{bpy})(\text{NCS})_2$.⁷ However, for both of these the iron coordination environments are axial. Finally, the metal-metal distance within the chain is estimated to be ~ 6 Å from consideration of the preceding polymer systems. X-ray patterns of other members of the $\text{M}(\text{bpy})(\text{NCS})_2$ series ($\text{M} = \text{Mn}, \text{Fe}, \text{Co}, \text{Ni}$, and Cu) show that several other members probably also have the same zigzag chain structure shown in Figure 7. These patterns indicate that $\text{Mn}(\text{bpy})(\text{NCS})_2$ and $\text{Co}(\text{bpy})(\text{NCS})_2$ are isomorphous to $\text{Fe}(\text{bpy})(\text{NCS})_2$. It will be shown in a future paper³⁴ that the spectral and magnetic properties of

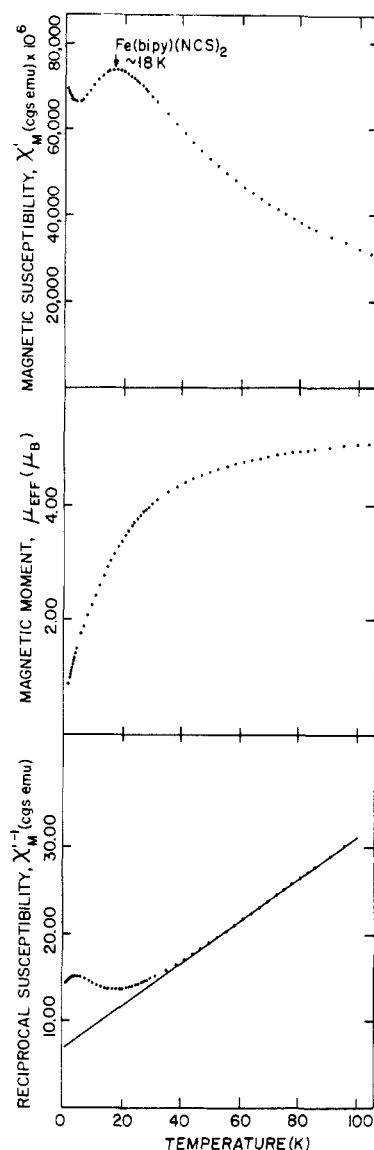


Figure 8. Plots of the magnetic data (χ_M' , $\chi_M'^{-1}$, and μ) for $\text{Fe}(\text{bpy})(\text{NCS})_2$ between 0 and 100 K with a magnetic field of 5.10 kG.

$\text{Mn}(\text{bpy})(\text{NCS})_2$ and $\text{Co}(\text{bpy})(\text{NCS})_2$ are also fully consistent with the zigzag-type structure proposed for $\text{Fe}(\text{bpy})(\text{NCS})_2$.

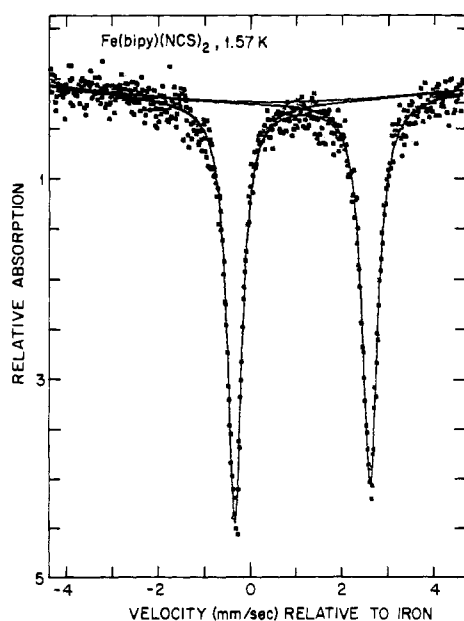
Magnetic Measurements. Magnetic susceptibility measurements for $\text{Fe}(\text{bpy})(\text{NCS})_2$ have been taken between 1.4 and 300 K for ten different magnetic fields varying from 1.6 to 5.1 kG and are found to be field independent. The data measured above 100 K do not obey a single Curie-Weiss law. However, this is not unexpected since $\text{Fe}(\text{bpy})(\text{NCS})_2$ clearly exists in two different structural phases in this temperature range. The remainder of this section will concentrate on the results for temperatures below 100 K for which there is only the single-phase LT form present. Figure 8 shows plots of the magnetic data (χ_M' , $\chi_M'^{-1}$, and μ) between 0 and 100 K for a field of 5.10 kG. The line in the $\chi_M'^{-1}$ vs. T plot is a least-squares fit based on a Curie-Weiss law with the parameters $\theta = -27.8$ K, $C = 4.10$ emu mol⁻¹, and $\mu_{\text{eff}} = 5.72$, done between 50 and 100 K. Table IV gives typical values of the susceptibility and moment in a field of 5.10 kG. The large negative value of θ and the broad maximum in χ_M at ~ 18 K indicate a relatively strong antiferromagnetic interaction between iron atoms. These antiferromagnetic interactions also result in a continuously decreasing moment down to ~ 1.4 K; see Figure 8. At $T \leq 18$ K, the susceptibility decreases in value, reaches a minimum, and then rises again. We believe that the latter is due to the onset of an additional

(33) L. Capacchi, G. F. Gasparri, M. Nardelli, and G. Peliezi, *Acta Crystallogr., Sect. B*, **B24**, 1199 (1968).

(34) B. W. Dockum and W. M. Reiff, to be submitted for publication.

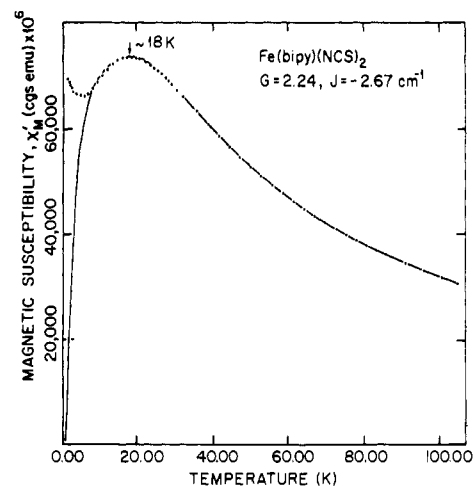
Table IV. Sample Magnetic Data for Fe(bpy)(NCS)₂^a

T, K	10 ⁶ χ _M '	μ _B	T, K	10 ⁶ χ _M '	μ _B
85.57	36 235	4.98	14.57	72 887	2.91
75.03	39 937	4.90	13.28	72 221	2.77
66.66	43 465	4.81	11.80	71 160	2.59
55.27	49 352	4.67	10.39	69 964	2.41
46.65	54 631	4.51	9.20	68 726	2.25
35.22	63 368	4.22	7.92	67 609	2.07
31.56	66 090	4.08	6.61	66 569	1.88
29.93	67 299	4.01	5.77	66 231	1.75
28.53	68 400	3.95	4.20	66 230	1.49
27.70	69 069	3.91	4.00	66 350	1.46
26.92	69 629	3.87	3.76	66 419	1.41
25.78	70 319	3.81	3.49	66 658	1.36
24.82	70 922	3.76	3.25	66 726	1.32
23.76	71 502	3.69	3.01	67 072	1.27
22.94	71 910	3.63	2.75	66 762	1.21
21.67	72 532	3.54	2.49	67 518	1.16
20.58	73 002	3.47	2.25	67 793	1.10
19.43	73 233	3.37	2.01	68 065	1.04
18.25	73 420	3.27	1.78	68 641	0.99
16.82	73 408	3.14	1.39	69 271	0.88
15.62	73 288	3.03			

^a For a magnetic field of 5.10 kG.Figure 9. Zero-field Mössbauer spectrum of Fe(bpy)(NCS)₂ at 1.57 K.

magnetic-structural phase transformation, the nature of which is uncertain at present. High-field vibrating-sample magnetometry results for the isomorphous Mn(bpy)(NCS)₂ indicate canted AF behavior at these low temperatures. The iron analogue is being further studied in this regard. A Mössbauer spectrum taken at 1.57 K shows a single quadrupole doublet; see Figure 9. This spectrum exhibits no magnetic hyperfine splitting or broadening and suggests that the Néel temperature and any three-dimensional cooperative magnetic ordering for Fe(bpy)(NCS)₂ occur at temperatures less than ~1.6 K.

The magnetic properties of low-dimensionality lattice systems, i.e., one-dimensional linear chain and two-dimensional layers, may be explained by using models such as the Heisenberg, XY, and Ising exchange models, which take into account long-range magnetic interactions along the chains or within the layers.³⁵ These models have been used to theoretically reproduce the essential features of the susceptibility of the linear chains Fe(N₂H₅)₂(SO₄)₂³⁶ and Fe(C₂O₄)₂·2H₂O.

Figure 10. Plot of χ_M' vs. T, which includes the results of the fit using the Heisenberg-Dirac-Van Vleck dipolar coupling model for $g = 2.24$, $J = -2.7 \text{ cm}^{-1}$, and $N\alpha = 0$.

O.^{37,38} However, in other magnetic systems, the magnetic dimensionality may be different from the lattice dimensionality. The compound Cu(NO₃)₂·2.5H₂O may be theoretically represented by negative exchange between pairs of copper atoms within the lattice.³⁹⁻⁴¹ A similar dimeric model has been used to interpret the magnetic properties of Cu(NH₃)₂CO₃,⁴² which has chains of copper atoms bridged by carbonate anions.⁴³ By analogy with the above copper systems, we have made an attempt to interpret the magnetic properties of Fe(bpy)(NCS)₂ using a pairwise, dimer model of interactions between iron atoms in view of the likelihood of the zigzag chain structure proposed for Fe(bpy)(NCS)₂ preventing (strong) long-range magnetic interactions. If this latter model is appropriate, it is possible to estimate the exchange energy, J , by fitting the magnetic susceptibility to the Heisenberg-Dirac-Van Vleck dipolar coupling model for a spin $S = 2$ system. The necessary equation is⁴⁴

$$\chi_M = \frac{Ng^2\mu_B^2}{3KT} \left[\frac{90 + 42e^{8x} + 15e^{14x} + 3e^{18x}}{9 + 7e^{8x} + 5e^{14x} + 3e^{18x} + e^{20x}} \right] + N\alpha \quad (1)$$

where $x = J/KT$ (J is the exchange energy, and $|2J|$ is the singlet-triplet splitting, and $N\alpha$ is the temperature-independent paramagnetism. The quantities N , g , μ_B , and k have their usual meanings. Figure 10 shows the plot of the experimental magnetic susceptibilities and those calculated from eq 1 with the values $g = 2.2$ and $J = -2.7 \text{ cm}^{-1}$ determined from a fit of the experimental data done between 5.73 and 303 K with $N\alpha = 0$. Even though the dipolar model gives a reasonable fit to the data below ca. 100 K, a single-phase region, the fit is based on two assumptions that may not be valid. The first

- (36) H. T. Witteveen and J. Reedijk, *J. Solid State Chem.*, **10**, 151 (1974).
 (37) S. deS Barros and S. A. Friedberg, *Phys. Rev.*, **141**, 637 (1966).
 (38) J. T. Wroblewski and D. B. Brown, *Inorg. Chem.*, **18**, 2738 (1979).
 (39) L. Berger, S. A. Friedberg, and J. T. Schriempf, *Phys. Rev.*, **132**, 1057 (1963).
 (40) S. A. Friedberg and C. A. Raquet, *J. Appl. Phys.*, **39**, 1132 (1968).
 (41) S. Wittekoek and N. J. Poulsen, *J. Appl. Phys.*, **39**, (1963).
 (42) D. Y. Jeter, D. J. Hodgson, and W. E. Hatfield *Inorg. Chem.*, **11**, 185 (1972).
 (43) M. Meyer, P. Singh, W. E. Hatfield, and D. J. Hodgson, *Acta Crystallogr., Sect. B*, **B28**, 1607 (1972).
 (44) W. Wojciechowski, *Inorg. Chim. Acta*, **1**, 319 (1967). Note: The susceptibility equations in this reference are for 1 mol of dimer and are derived by using the Hamiltonian $-JS_1 \cdot S_2$, giving a singlet-triplet splitting of $|J|$. Equation 1 of this work is based on 1 mol of metal and may be obtained from the equations in the above reference by multiplying them by $3/2$ and replacing each x by $2x$.

is that zero-field splitting effects are small, implying an isotropic g value close to 2. In high-spin iron(II) compounds, the zero-field effects can be large (comparable in magnitude to the intracenter exchange interactions) resulting in an anisotropic g tensor. The dipolar coupling model does not include the zero-field effects directly but incorporates them indirectly in the g value. This may be the reason the g value obtained from the fit ($g = 2.2$) is greater than 2. It was also assumed the intercluster (pair in the present case) exchange was zero. In real systems, the intercluster interactions are operable but are usually considerably weaker than the intracenter interactions justifying the preceding assumption. It is interesting to note that a spin-coupled dimer model has been used in the interpretation of the magnetic data in a recent study of the linear chain polymer $\text{Fe}(\text{C}_2\text{O}_4)\cdot 2\text{H}_2\text{O}$.³⁸ In this study, the magnetic susceptibility exhibited a single broad maximum at ~ 35 K and could be represented accurately by a 1-D Heisenberg model for $T > 25$ K. Below 25 K, the susceptibility dropped sharply, which was interpreted as the onset of 3-D antiferromagnetic ordering. An alternative fit with the Heisenberg-Dirac-Van Vleck dipolar coupling model gave a successful fit of the data for $T > 4.2$ K, perhaps suggesting significant pairwise antiferromagnetic interactions between metal atoms.

More complete theories which incorporate the foregoing interpair interactions are known as the ladder⁴⁵ and the alternating chain models.⁴⁶ In the former model, the strongest interactions occur *between metal atoms in adjacent polymer chains* with weaker interactions within the chain. The stronger

interactions from the "rungs", and the weaker interactions from the "sides" of the ladder. In contrast, in the alternating chain model, the strong intrapair and weaker interpair interactions *alternate throughout* the chain. Both models have been used to explain the magnetic properties of $\text{Cu}(\text{NO}_3)_2\cdot 2.5\text{H}_2\text{O}$.⁴⁷ The available data are in agreement with the alternating chain model. We tend to reject the ladder model for $\text{Fe}(\text{bpy})(\text{NCS})_2$ in view of the proposed structure and analogy to $\text{Co}(\text{bpy})\text{Cl}_2$. For the latter compound,¹² there are no bonded interactions between parallel chains, and the *closest interchain* Co-Co and Cl-Cl distances are 8.8 and 6.7 Å, respectively; i.e., the rungs are very weak or nonexistent. It does not seem likely that some form of an alternating chain model is most appropriate to represent the magnetic behavior of $\text{Fe}(\text{bpy})(\text{NCS})_2$. However, in the final analysis, this can only be judged in the light of an X-ray structure determination. In any event, to our knowledge, theoretical work using the alternating chain model has been done only for $S = 1/2$,⁴⁷ and verification of this model in the present case must await advances in the theory of the alternative chain. In subsequent work, we shall report on the antiferromagnetic behavior of $\text{Mn}(\text{bpy})(\text{NCS})_2$ and the strong 3-D ferromagnetism of the divalent nickel analogue.

Acknowledgment. We wish to acknowledge the support of the National Science Foundation, Division of Materials Research, Solid State Chemistry Program, Grants No. DMR-77-12625 and DMR-80-16441.

Registry No. $\text{Fe}(\text{bpy})(\text{NCS})_2$, 79803-24-0; $\text{Fe}(\text{bpy})_2(\text{NCS})_2$, 37843-42-8.

(45) J. C. Bonner and S. A. Friedberg, *AIP Conf. Proc.*, No. 18 (2), 1311 (1973).

(46) W. Duffy, Jr., and K. P. Barr, *Phys. Rev.*, **165**, 647 (1968).

(47) J. Eckert, D. E. Cos, G. Shirane, S. A. Friedberg, and H. Kobayashi, *Phys. Rev. B: Condens. Matter*, **20**, 4596 (1979), and references within.

Contribution from the Institute for Materials Research and Department of Chemistry, McMaster University, Hamilton, Ontario, Canada L8S 4M1

Magnetic Properties of $\alpha\text{-Li}_2\text{Eu}_5\text{O}_8$ and $\beta\text{-Li}_2\text{Eu}_5\text{O}_8$. Evidence for Linear-Chain Heisenberg Ferromagnetic Behavior

TABELLO NYOKONG and J. E. GREEDAN*

Received February 4, 1981

Some magnetic properties of the α and β modifications of $\text{Li}_2\text{Eu}_5\text{O}_8$ have been determined in the temperature range 1.2–50 K. In both materials there occur linear chains of Eu^{II} ions at rather close distances, 3.5 Å, while the interchain distances are much greater, 7.72 Å for the α phase and 8.57 Å for the β phase. Susceptibility data between 4.2 and 50 K can be analyzed in terms of a linear-chain Heisenberg ferromagnetic model for both compounds. Both phases undergo 3-D AF order with $T_N = 2.2$ K for the α phase and 1.9 K for the β phase. Metamagnetic transitions are observed at critical fields of 0.019 T for the α phase and 0.010 T for the β phase. Intra-, J_1 , and interchain, J_2 , exchange parameters have been derived as follows: α phase $J_1/k = +0.2$ K, $J_2/k = -0.002$ K; β phase $J_1/k = +0.1$ K, $J_2/k = -0.001$ K. The values of J_1 are discussed in light of diffuse-reflectance spectra for both phases and current ideas about exchange in Eu^{2+} compounds.

Introduction

Very few compounds exist whose magnetic behavior is a good approximation to the ferromagnetic linear (1-D) Heisenberg chain. To date the best examples are Cu^{II} ($S = 1/2$) and Ni^{II} ($S = 1$) salts such as $[(\text{CH}_3)_4\text{N}]\text{NiCl}_3$ ¹ and $[(\text{C}_6\text{H}_5)_4\text{N}]\text{CuCl}_3$.² Compounds containing divalent europium, Eu^{II} , seem to have been overlooked as potential candidates. Eu^{II} , $^8\text{S}_{7/2}$, is an ideal Heisenberg ion, which, given the spin

value of $7/2$, should represent a fair approximation to classical $S = \infty$ behavior. Furthermore, ferromagnetic exchange interactions are commonly found in Eu^{II} compounds with relatively short $\text{Eu}^{\text{II}}\text{-Eu}^{\text{II}}$ distances. It is well-known that EuO , with a near neighbor (nn) $\text{Eu}^{\text{II}}\text{-Eu}^{\text{II}}$ distance of 3.63 Å, has a ferromagnetic nn interaction, $J_1/k = +0.5$ K.³

The magnetic properties of Eu_2O_4 ($\text{Eu}^{\text{II}}\text{Eu}^{\text{III}}\text{O}_4$) have been determined by Holmes and Schieber.⁴ In this compound the

(1) B. C. Gerstein, F. D. Gehring, and R. D. Willett, *J. Appl. Phys.*, **43**, 1932 (1972).

(2) C. P. Landee and R. D. Willett, *Phys. Rev. Lett.*, **43**, 463 (1979).

(3) N. Menyuk, K. Dwight, and T. B. Reed, *Phys. Rev. B: Solid State*, **3**, 1689 (1971).

(4) L. Holmes and Schieber, *Phys. Rev.*, **167**, 450 (1968).